

# Temperature dependence of Auger recombination in highly injected crystalline silicon

Sisi Wang and Daniel Macdonald

Research School of Engineering, College of Engineering and Computer Science, The Australian National University, Canberra ACT 0200, Australia

(Received 12 August 2012; accepted 7 November 2012; published online 6 December 2012)

The Auger lifetime in crystalline silicon has been measured under high injection conditions using an injection- and temperature-dependent photoconductance apparatus, across a temperature range from 243 to 473 K (−30 to 200 °C). The corresponding ambipolar Auger coefficient was found to have a value of  $1.6 \times 10^{-30} \text{ cm}^6/\text{s}$  at 303 K (30 °C) at an injection level of  $5 \times 10^{16} \text{ cm}^{-3}$ . The Auger coefficient was found to decrease between 243 K and 303 K, and then remain approximately constant up to 473 K. An empirical parameterization of the measured ambipolar Auger coefficient is provided. © 2012 American Institute of Physics. [<http://dx.doi.org/10.1063/1.4768900>]

Auger recombination is an intrinsic recombination process that can influence the performance of silicon devices such as solar cells. It is a three particle process in which an electron and a hole recombine, giving the excess energy to a third free carrier. There have been numerous studies of Auger recombination in crystalline silicon, including the impact of Coulomb-enhancement effects.<sup>1–9</sup> However, these have mostly been performed at room temperature. There is little data published on the temperature dependence of Auger recombination in silicon, despite the fact that devices such as solar cells often operate at temperatures above or below room temperature.

Neglecting Coulomb-enhancement effects, the Auger recombination rate is given by  $R_{\text{Auger}} = C_n n^2 p + C_p n p^2$ , where  $n$  and  $p$  are the electron and hole concentrations and  $C_n$  and  $C_p$  are the electron and hole Auger coefficients.<sup>5</sup> Under high injection conditions, with excess electron and hole densities  $\Delta n = \Delta p$ , the Auger lifetime  $\tau_{\text{Auger}}$  can be expressed as  $1/\tau_{\text{Auger}} = C_a \Delta p^2$ , where  $C_a$  is the ambipolar Auger coefficient.

In general, however, the ambipolar Auger coefficient has a mild dependence on the injection level, due to Coulomb-enhancement effects.<sup>5,9</sup> Kerr and Cuevas<sup>9</sup> proposed an empirical expression for the injection level dependent ambipolar Auger coefficient  $C_a^* = 3 \times 10^{-27} \Delta p^{-0.2}$ , valid at room temperature for excess carrier densities greater than  $3 \times 10^{15} \text{ cm}^{-3}$ .

In this article, we investigate the impact of temperature on the ambipolar Auger coefficient under high injection. The sample studied was a 3 Ω cm p-type boron-doped wafer with a thickness of 0.0421 cm, grown by the float-zone method. The boron doping concentration was  $5 \times 10^{15} \text{ cm}^{-3}$ , ensuring that carrier lifetime measurements at excess carrier densities at  $5 \times 10^{16} \text{ cm}^{-3}$  and above would be in high injection. The surfaces of the wafer were passivated by plasma-enhanced chemical vapour deposited silicon nitride films to suppress surface recombination.<sup>10</sup> The equipment used for the lifetime measurements is a modified temperature- and injection-dependent quasi-steady-state photoconductance (QSSPC) carrier lifetime apparatus.<sup>11,12</sup> Here, we studied a temperature range from 243 to

473 K (−30 to 200 °C), over which we could ensure accurate temperature control, and also be confident that the potential negative impact of non-uniform carrier profiles throughout the wafer thickness could be avoided, as described below.

A crucial aspect of temperature dependent photoconductance-based lifetime measurements is the calibration of the inductive coil as a function of temperature.<sup>12,13</sup> We used thirteen wafers with known conductance values at room temperature ranging from 0.0162 to 0.4425 Siemens. We have used Klaassen's mobility model<sup>14,15</sup> to calculate the conductance of these wafers at other temperatures, assuming that there were no carrier freeze-out effects across the temperature range studied.

At each temperature, the relationship between the measured coil voltage  $V$  and the conductance  $\sigma$  of the calibration wafers can be parameterized with the quadratic expression  $\sigma = a(T)V^2 + b(T)V$ , as is customary for this type of lifetime measurement device. Here, the quadratic pre-factor  $a$  and the linear pre-factor  $b$  may, in general, be temperature dependent. Figure 1 shows the measured values of  $a$  and  $b$  as a function of temperature. The quadratic pre-factor  $a$  was found to

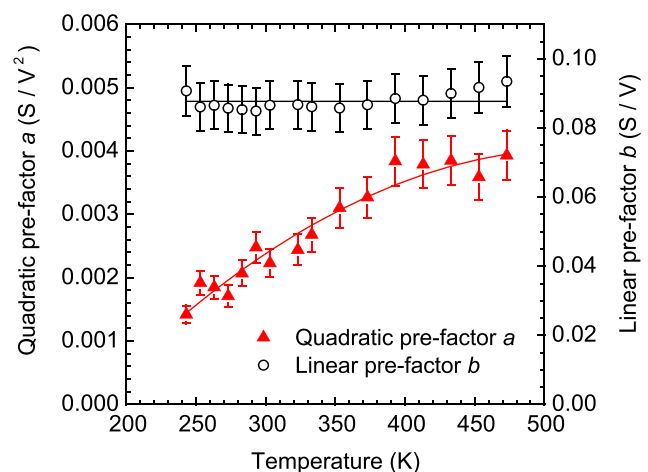


FIG. 1. Temperature dependence of the quadratic and linear pre-factors,  $a$  and  $b$  respectively, of the inductive coil apparatus used for measuring carrier lifetimes.

be quite strongly temperature dependent, while  $b$  was essentially unchanged, within the experimental uncertainty. Therefore, a constant value of  $b = 0.0877 \text{ S/V}$  was used in this work, while for  $a$ , we used an empirical fit to the data of  $a = -3.21 \times 10^{-8} T^2 + 3.39 \times 10^{-5} T + 0.0049$  (in units of  $\text{S/V}^2$ , with  $T$  in Kelvin). This fit is shown as a solid line in Figure 1. Note that for high injection lifetime measurements, as are required here, the quadratic pre-factor has a greater impact than at lower injection levels.

Using these calibration constants, the effective carrier lifetimes of the p-type sample were measured as a function of temperature, at excess carrier densities between  $1 \times 10^{16} \text{ cm}^{-3}$  and  $7 \times 10^{16} \text{ cm}^{-3}$ , with the achievable upper excess carrier density depending on the lifetime. Klaassen's mobility model was used to determine the injection- and temperature-dependent mobility sum required for the calculation of the carrier lifetime and average excess carrier density from the photoconductance data.<sup>11,14,15</sup> This model was chosen since the standard model employed in the QSSPC analysis does not include temperature dependence, and the model of Reggiani *et al.*,<sup>16</sup> which has been used before for low-injection temperature-dependent lifetime measurements,<sup>12,17</sup> is not suited for high injection conditions.

The results are shown in Figure 2 for an excess carrier density of  $5 \times 10^{16} \text{ cm}^{-3}$ , a value for which we could extract lifetime data at all temperatures studied. Considering uncertainties in the calibration constants and other sources,<sup>18</sup> we estimate the uncertainty in the measured lifetime values to be  $\pm 15\%$ . Data from the parameterization of Kerr and Cuevas<sup>9</sup> at 300 K are also shown, as well as measured data from Yablonovitch and Gmitter<sup>19</sup> and Schmidt *et al.*<sup>8</sup> taken at the same excess carrier density. The measured lifetimes are in good agreement with the literature values near room temperature. The high injection lifetime was found to be mildly temperature dependent, increasing between 243 K and room temperature, and then remaining approximately constant up to 473 K.

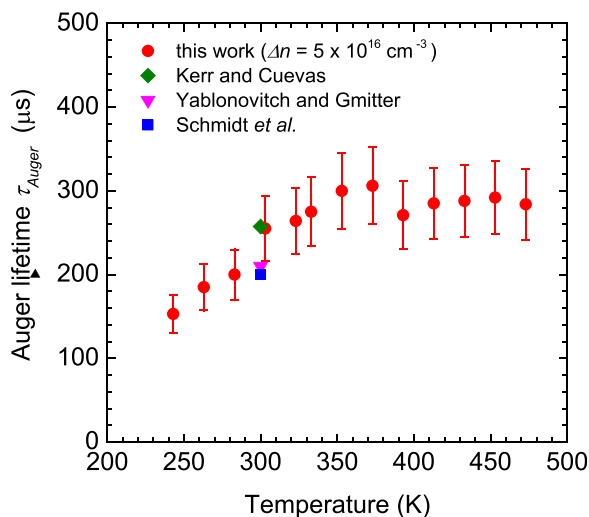


FIG. 2. Temperature dependence of the Auger lifetime measured at an injection level of  $5 \times 10^{16} \text{ cm}^{-3}$ . Data from Kerr and Cuevas' parameterization<sup>9</sup> and measured values from Yablonovitch and Gmitter<sup>19</sup> and Schmidt *et al.*<sup>8</sup> at 300 K are also shown.

The agreement with the values from the literature indicates that the measured effective lifetimes are dominated by Auger recombination, as expected at this injection level. However, at this point, it is important to address the potential impact of possible measurement artefacts that could affect the data.

First, an underlying assumption in the lifetime measurement method is that the carrier concentrations in the samples are almost uniform as a function of depth. As both the carrier lifetime and the ambipolar diffusion coefficient are temperature dependent, the validity of this assumption should be considered. At 303 K, using an ambipolar diffusivity<sup>14,15,20</sup> of  $13.4 \text{ cm}^2/\text{s}$  at an excess carrier density of  $5 \times 10^{16} \text{ cm}^{-3}$ , combined with the measured excess carrier lifetime of  $250 \mu\text{s}$ , yields an ambipolar carrier diffusion length of  $580 \mu\text{m}$ . The corresponding carrier profile as a function of depth has been simulated using the QSS-MODEL software,<sup>21,22</sup> under AM1.5G illumination, as shown in Figure 3. This reveals only a small change in the carrier density throughout the wafer thickness, from a maximum of  $5.7 \times 10^{16} \text{ cm}^{-3}$  at the front to a minimum of  $4.7 \times 10^{16} \text{ cm}^{-3}$  at the rear, with an average value of  $5.0 \times 10^{16} \text{ cm}^{-3}$ . These minor carrier density variations do not significantly impact the measured Auger lifetime, as evidenced by the good agreement with the literature data at 300 K in Figure 2.

At 243 K, with a lifetime of  $150 \mu\text{s}$ , the ambipolar carrier diffusion length drops to around  $470 \mu\text{m}$ , with the corresponding excess carrier profile shown in Figure 3. Again the variations in the excess carrier densities are small (from  $6.0 \times 10^{16} \text{ cm}^{-3}$  to  $4.5 \times 10^{16} \text{ cm}^{-3}$ ). Profiles are also shown for 263 K and 473 K in Figure 3, confirming that in all cases reported here, variations in the excess carrier density are minor. These considerations affect the range of injection levels over which the Auger lifetime can be accurately measured. At average excess carrier densities approaching  $10^{17} \text{ cm}^{-3}$ , the carrier profiles become increasingly non-uniform due to the reduced lifetime. This can be countered by using thinner wafers, although this then increases the possible impact of surface recombination, as described below. Consequently, we

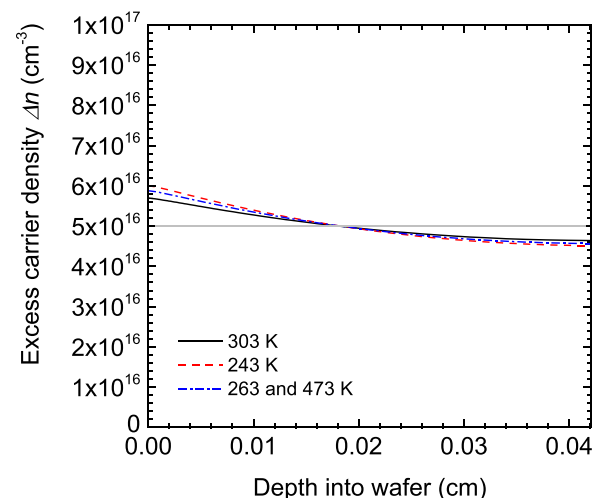


FIG. 3. Modeled excess carrier density as a function of depth into the wafer, for temperatures of 243, 263, 303, and 473 K. The horizontal grey line indicates the average excess carrier density of  $5 \times 10^{16} \text{ cm}^{-3}$ .

have restricted ourselves to reporting the Auger lifetime at an average excess carrier density of  $5 \times 10^{16} \text{ cm}^{-3}$  in this work.

Another important aspect is the possible impact of surface recombination on the measured lifetimes. A convenient method of testing for this effect is to measure samples of different thickness. The data shown in Figure 2 are for a relatively thick wafer ( $W = 0.0421 \text{ cm}$ ), however we also measured a significantly thinner sample ( $W = 0.0274$ ) across the temperature range studied here. Any significant impact of surface recombination would manifest itself as a reduced lifetime in the thinner sample. However, within experimental error, we did not observe a reduced lifetime in the thinner sample across the temperature range examined. We, therefore, conclude that surface recombination does not play a significant role in the reported lifetimes.

This conclusion is corroborated by the following estimates of the expected impact of surface recombination at room temperature. While it is difficult to directly measure the surface recombination velocity (SRV) of the passivating SiN films at an excess carrier density of  $5 \times 10^{16} \text{ cm}^{-3}$ , precisely because the effective lifetimes are dominated by Auger recombination, the SRV can be estimated more accurately at an excess carrier density of  $10^{16} \text{ cm}^{-3}$ , above which it should not be strongly injection dependent according to Shockley read Hall (SRH) statistics. For the doping level used here, the corresponding upper limit on the SRV is  $S = 5 \text{ cm/s}$  at room temperature.<sup>10</sup> This yields an effective “surface lifetime” ( $W/2S$ ) of 4.2 ms for our thick sample, which would contribute only 6% to the measured lifetime of  $250 \mu\text{s}$  at  $5 \times 10^{16} \text{ cm}^{-3}$ . Even for the thinner sample, the impact would be 10% at most. This confirms that surface recombination has a negligible impact on the measured Auger lifetime at room temperature. The fact that the measured lifetimes in the thick and thin samples were within the experimental uncertainty of each other allows us to conclude the same at other temperatures.

Once satisfied that the measured lifetimes indeed represent the Auger lifetime, the ambipolar Auger coefficient  $C_a$  can be determined via the expression  $1/\tau_{\text{Auger}} = C_a \Delta p^2$ , as a function of temperature. The result is plotted in Figure 4, which also shows some literature values<sup>3,4,6,9,19,23</sup> of the ambipolar Auger coefficient in silicon, which were determined over excess carrier density ranges that included  $5 \times 10^{16} \text{ cm}^{-3}$ , and at room temperature. Jonsson *et al.*<sup>6</sup> reported values at 300 and 363 K. In general, our measured data are in good agreement with these literature values, keeping in mind that in several cases, the exact injection level was not clearly specified. There have been numerous other published values obtained near room temperature, as summarized elsewhere.<sup>6,9</sup> However, these were determined at significantly different injection levels, meaning they are not directly comparable to our data due to the impact of Coulomb-enhancement effects, or other injection level effects.<sup>9</sup> There is little published data on the temperature dependence of the ambipolar Auger coefficient in silicon. Results reported by Huld *et al.*<sup>2</sup> across the temperature range 195–372 K showed a monotonic increase with temperature that could be fitted with a  $T^{0.6}$  dependence. However, in contrast, data from Dziewior and Schmid<sup>1</sup> at 77, 300, and 400 K showed only a weak temperature dependence. Their

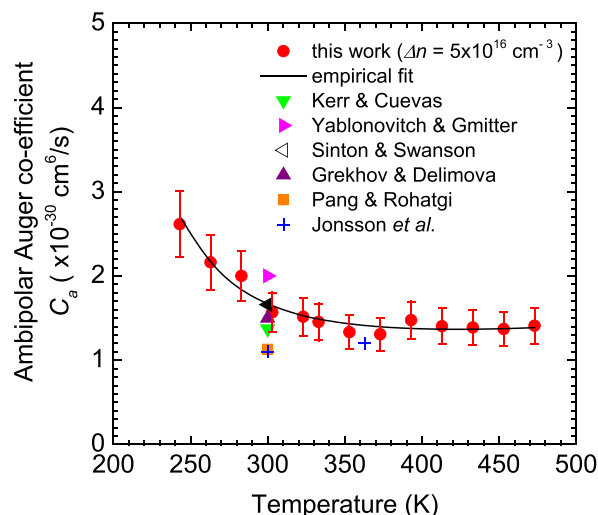


FIG. 4. Temperature dependence of the ambipolar Auger coefficient  $C_a$  determined at an injection level of  $5 \times 10^{16} \text{ cm}^{-3}$ . An empirical fit to the data, given in the text, is shown as a solid line. Also shown are literature values Kerr and Cuevas,<sup>9</sup> Yablonovitch and Gmitter,<sup>19</sup> Sinton and Swanson,<sup>3</sup> Grekhov and Delimova,<sup>23</sup> Pang and Rohatgi,<sup>4</sup> and Jonsson *et al.*<sup>6</sup>

values were measured at higher injection levels than used here. As shown in Figure 4, our own data are in good agreement with the result from Jonsson *et al.* at 363 K, for which the excess carrier density was specified as  $5 \times 10^{16} \text{ cm}^{-3}$ , while their value at 300 K was not as clearly defined in terms of injection level.

We have parameterized our temperature dependent ambipolar Auger coefficient data, as shown in Figure 4. The resulting expression, valid for excess carrier densities of  $5 \times 10^{16} \text{ cm}^{-3}$ , is (with  $T$  in Kelvin)

$$C_a = \frac{1.1 \times 10^{-28}}{T - 193} + 2.1 \times 10^{-33} T. \quad (1)$$

This parameterization is not based on any physically predicted temperature dependence, since our data cannot be fitted either with a single activation energy, as expected for phononless processes, or with a single phonon energy for phonon-assisted transitions.<sup>2</sup> This implies that a more complex model for the temperature dependence of Auger recombination is required. The expression above is only valid over the temperature range of 243–473 K. The effect of Coulomb-enhancement may be included to generalize this expression to other injection-levels, for example, by including the injection-dependent factor determined by Kerr and Cuevas for injection levels above  $3 \times 10^{15} \text{ cm}^{-3}$ . This can be achieved by multiplying the above expression by  $[\Delta p/(5 \times 10^{16})]^{-0.2}$ . Note however that the value of the exponent,  $-0.2$ , may, in general, be temperature dependent also.

In conclusion, Auger lifetimes in crystalline silicon were measured at an injection level of  $5 \times 10^{16} \text{ cm}^{-3}$ , over the temperature range from 243 to 473 K ( $-30$  to  $200^\circ\text{C}$ ). These values were used to calculate the ambipolar Auger coefficient, which was found to decrease between 243 K and 303 K, and then remain approximately constant at higher temperatures. The value at room temperature was found to be in reasonable agreement with commonly used literature values taken at the

same injection level. An empirical expression for the temperature dependence of the ambipolar Auger coefficient has been determined, since simple physical models could not describe the observed temperature dependence. This empirical expression may be useful in device modelling.

This work has been supported by the Australian Research Council. The authors are grateful to Fiacre Rougieux for assisting with calibration of the inductive coil.

- <sup>1</sup>J. Dziewior and W. Schmid, *Appl. Phys. Lett.* **31**, 346 (1977).
- <sup>2</sup>L. Hultdt, N. G. Nilsson, and K. G. Svantesson, *Appl. Phys. Lett.* **35**, 776 (1979).
- <sup>3</sup>R. A. Sinton and R. M. Swanson, *IEEE Trans. Electron Devices* **ED-34**, 1380 (1987).
- <sup>4</sup>S. K. Pang and A. Rohatgi, *Applied Physics Lett.* **59**, 195 (1991).
- <sup>5</sup>P. P. Altermatt, J. Schmidt, G. Heiser, and A. G. Aberle, *J. Appl. Phys.* **82**, 4938 (1997).
- <sup>6</sup>P. Jonsson, H. Bleichner, M. Isberg, and E. Nordlander, *J. Appl. Phys.* **81**, 2256 (1997).
- <sup>7</sup>S. W. Glunz, D. Biro, S. Rein, and W. Warta, *J. Appl. Phys.* **86**, 683 (1999).
- <sup>8</sup>J. Schmidt, M. J. Kerr, and P. P. Altermatt, *J. Appl. Phys.* **88**, 1494 (2000).
- <sup>9</sup>M. J. Kerr and A. Cuevas, *J. Appl. Phys.* **91**, 2473 (2002).
- <sup>10</sup>M. J. Kerr and A. Cuevas, *Semicond. Sci. Technol.* **17**, 166 (2002).
- <sup>11</sup>R. A. Sinton and A. Cuevas, *Appl. Phys. Lett.* **69**, 2510 (1996).
- <sup>12</sup>B. B. Paudyal, K. R. McIntosh, D. H. Macdonald, B. S. Richards, and R. A. Sinton, *Prog. Photovoltaics* **16**, 609 (2008).
- <sup>13</sup>J. Schmidt, *Appl. Phys. Lett.* **82**, 2178 (2003).
- <sup>14</sup>D. B. M. Klaassen, *Solid-State Electron.* **35**, 953 (1992).
- <sup>15</sup>D. B. M. Klaassen, *Solid-State Electron.* **35**, 961 (1992).
- <sup>16</sup>S. Reggiani, M. Valdinoci, L. Colalongo, M. Rudan, G. Baccarani, A. D. Stricker, F. Illien, N. Felber, W. Fichtner, and L. Zullino, *IEEE Trans. Electron Devices* **49**, 490 (2002).
- <sup>17</sup>B. B. Paudyal, K. R. McIntosh, and D. H. Macdonald, *J. Appl. Phys.* **105**, 124510 (2009).
- <sup>18</sup>K. R. McIntosh and R. A. Sinton, in *Proceedings 23rd European Photovoltaic Solar Energy Conference, Valencia, Spain* (WIP-Renewable Energies, 2008), p. 77.
- <sup>19</sup>E. Yablonovitch and T. Gmitter, *Appl. Phys. Lett.* **49**, 587 (1986).
- <sup>20</sup>M. Rosling, H. Bleichner, P. Jonsson, and E. Nordlander, *J. Appl. Phys.* **76**, 2855 (1994).
- <sup>21</sup>A. Cuevas and R. Sinton, in *22nd European Photovoltaics Solar Energy Conference, Milan, Italy* (WIP-Renewable Energies, 2007), p. 38.
- <sup>22</sup>A. Cuevas and R. A. Sinton, in *Proceedings 23rd European Photovoltaic Solar Energy Conference, Valencia, Spain* (WIP-Renewable Energies, 2008), p. 315.
- <sup>23</sup>I. V. Grekhov and L. A. Delimova, *Sov. Phys. Semicond.* **14**, 529 (1980).